

Control Sideband Generation for Dual-Recycled Laser Interferometric Gravitational Wave Detectors

**B W Barr[†], O Miyakawa[‡], S Kawamura[§], A J Weinstein[‡], R Ward[‡],
S Vass[‡] and K A Strain[†]**

[†]Department of Physics and Astronomy, University of Glasgow, Glasgow, G12 8QQ, UK

[‡]LIGO Laboratory, California Institute of Technology, Pasadena, CA 91125, USA

[§]National Astronomical Observatory of Japan, Tokyo 181 8588, Japan

E-mail: b.barr@physics.gla.ac.uk

Abstract. We present **the problems** associated with generation of multiple control sidebands for length sensing and control of dual-recycled cavity-enhanced Michelson interferometers and the motivation behind more complicated sideband generation methods. We focus on the Mach Zehnder interferometer as a topological solution to the problem and present results from tests carried out at the Caltech 40 m prototype gravitational wave detector. The consequences for sensing and control for advanced interferometry are discussed, as are the implications for future interferometers such as Advanced LIGO.

PACS numbers: 42.60.-v, 42.60.Fc

There are several large scale projects around the world building and operating laser interferometric gravitational-wave detectors including LIGO [1] (USA), GEO600 [3] (UK/Germany), VIRGO [2] (France/Italy) and TAMA [4] (Japan). These detectors are based around enhanced Michelson interferometer optical topologies and operate by detecting fluctuations in optical phase produced by the relative displacement of mirrors responding to gravitational radiation.

These first generation detectors are expected to open up the field of gravitational wave astronomy with a detection event rate of up to a few events per year. The second generation of detectors are being developed to improve the peak gravitational wave detection sensitivity by more than an order of magnitude and improve the expected event rate by several orders of magnitude [5]. These advanced detectors will incorporate several enhancements over the basic Michelson design and will have the general form shown in Figure 1. The interferometer has a specific operating condition requiring the relative lengths between optics to be sensed and controlled. The final sensing and control scheme for the Advanced LIGO [6] detectors is currently being investigated using the Caltech 40 m prototype system.

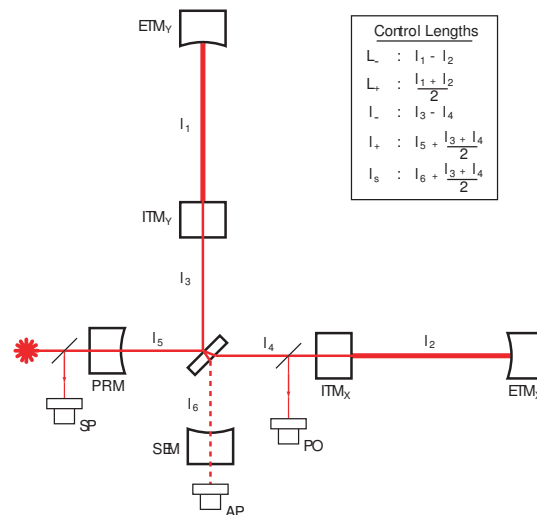


Figure 1. General form of the Advanced LIGO detectors and the 40 m prototype system. The logical control lengths (or degrees of freedom) L_- , L_+ , L_- and L_+ are shown, and the 3 possible points for signal detection are identified as SP (symmetric port), AP (antisymmetric port), and PO (pick-off port).

The sensing and control scheme being considered for this system has been discussed in detail [7] and is an extrapolation from the well-known Pound-Drever-Hall reflection locking scheme [8] where phase modulation sidebands are imposed on the laser light (carrier). After interaction with the interferometer the light is detected at all three detection ports and the signals are demodulated to give a bipolar control signal for each degree of freedom.

With five degrees of freedom and only three available detection points the sensing and control scheme being investigated requires the use of two sets of phase-modulated control sidebands (at frequencies f_1 and f_2). In the 40 m system $f_2 = 5f_1$ where $f_1 = 33.033$ MHz. For Advanced LIGO the proposed values of f_1 and f_2 are 9 MHz and 180 MHz respectively,

where these frequencies depend on the interferometer topology and will give improved decoupling between sensing signals than is possible with the 40 m system. The sensing signals chosen to control the central part of the interferometer (lengths l_p , l_- and l_s) are derived from the beat signals ($f_1 \pm f_2$) between the sidebands (at ports SP, AP and PO respectively). The arm cavity sensing signals are derived from demodulation of the beat between one of the sidebands and the carrier using f_2 at AP to sense L_- (the gravitational wave detection length) and f_1 at SP to sense L_+ . One of the primary advantages of this double demodulation sensing method is the decoupling of the central degrees of freedom from the arm cavities.

At the desired operating point the arm cavities (L_- and L_+) and power recycling cavity (l_p) must be held on resonance with the incident carrier light, the output port must be held to a dark carrier fringe (l_-) and the signal recycling cavity (l_s) must be held to a specific resonance condition determined by the desired frequency response [7]. The control sidebands also resonate within the system to allow generation of length sensing signals. In the 40 m system, both sets of sidebands (at $\pm f_1$ and $\pm f_2$) are resonant in the power recycling cavity, while only one sideband (at $+f_2$) is resonant in the detuned signal recycling cavity. This unbalanced sideband system means that, while the interferometer is held to the operating point, different sidebands have different responses to the motion of different mirrors. Through careful selection of demodulation phase for each double demodulation signal, the coupling between the length sensing signals for l_p , l_- and l_s can be minimised. Since the central part of the interferometer is already decoupled from the arm cavities the sensing scheme for the system is optimally decoupled at the operating point, resulting in a roughly diagonal control matrix.

Double demodulation presents an additional difficulty with regard to the sideband generation requirements for advanced interferometer control. Generation via phase modulation of one set of sidebands of amplitude β at frequency f_2 on top of another set of amplitude α at frequency f_1 will impose additional sets of sidebands offset from the carrier (amplitude 1) at frequencies $f_1 \pm f_2$ with amplitude $\alpha\beta$. This effect can be seen in Figure 2 and has been termed 'sidebands on sidebands'. A signal produced by the beat between sidebands on sidebands and the carrier will result in a signal ($\alpha\beta \times 1 = \alpha\beta$) of the same magnitude as one derived from the beat between sidebands ($\alpha \times \beta = \alpha\beta$). Modeling of this system indicates that due to the high finesse of the arm cavities, the arm cavity degrees of freedom will not only be strongly coupled with the central part of the interferometer, but will actually be the dominant elements of the sensing signals for the central degrees of freedom. A sideband generation scheme must be used which does not result in sidebands of sidebands being present on the light. One such scheme is to use parallel modulators in a Mach Zehnder interferometer configuration (see right hand configuration in Figure 2). The Mach Zehnder interferometer as built at the 40 m lab is shown in Figure 3.

The Mach Zehnder configuration solves the problem of sidebands on sidebands, but for the purposes of high sensitivity interferometry the beams in each arm must be recombined in phase. Residual deviations from the desired recombination phase will introduce noise into the system and limit the interferometer detection sensitivity.

These residual motions were extensively modeled with respect to the effect on the

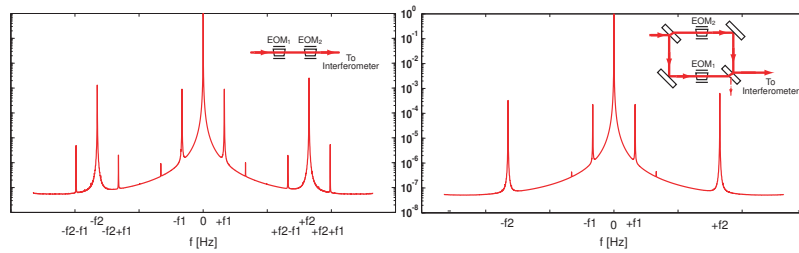


Figure 2. The left hand diagram shows the frequency components of the light with sidebands of sidebands as generated by a conventional series modulator configuration. The right hand side shows the required frequency components for a viable double demodulation sensing and control scheme as generated using a **parallel modulator** configuration.

L_- signal using the FINESSE interferometer simulation program [9]. An imbalanced interferometer will give greater coupling of laser noise to the control signals so the system was modeled with differences between the ITM transmissions of up to $\pm 10\%$. This represents the maximum imbalance expected in the 40 m system. A more balanced system will have less susceptibility to noise coupling to the L_- output signal.

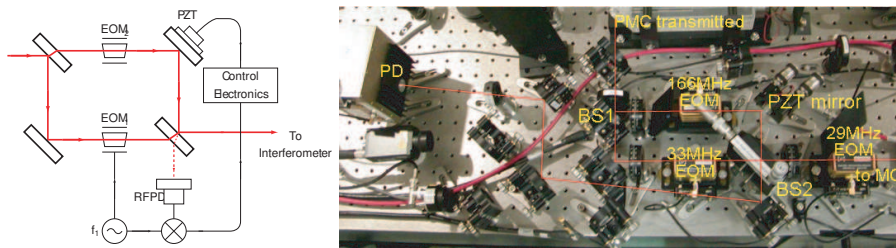


Figure 3. Left - Mach Zehnder control loop. Right - physical arrangement on the laser bench. The signal at the the RF photodiode (RFPD) is demodulated to provide a length sensing signal. This signal is fed back to the PZT in the f_2 arm to control the relative arm lengths, keeping the RFPD port dark for the carrier light.

Noise can be introduced in two main ways, namely common mode and differential mode fluctuations of the two Mach Zehnder arm lengths [10]. Differential arm length fluctuations couple directly to the L_- signal and will also result in fluctuations in the relative phase between the sidebands at f_1 and f_2 . Modeling of the system gives the coupling factor for differential Mach Zehnder arm motion to L_- motion as around 10^{-6} for a $\pm 10\%$ difference between ITM's. In contrast, common mode arm length fluctuations couple indirectly through other control systems - in this case the strongest indirect coupling mechanism is via the laser frequency stabilization servo loop. Modeling gives the coupling factor for common Mach Zehnder arm motion to L_- motion as around 10^{-7} for a $\pm 10\%$ difference between ITM's. The dominant mechanism for noise coupling is therefore direct coupling of differential Mach Zehnder arm length fluctuations to the L_- output signal.

A servo loop (shown in Figure 3) is used to hold the relative arm lengths of the Mach Zehnder constant and maintain the phase relationship between the sets of sidebands. The

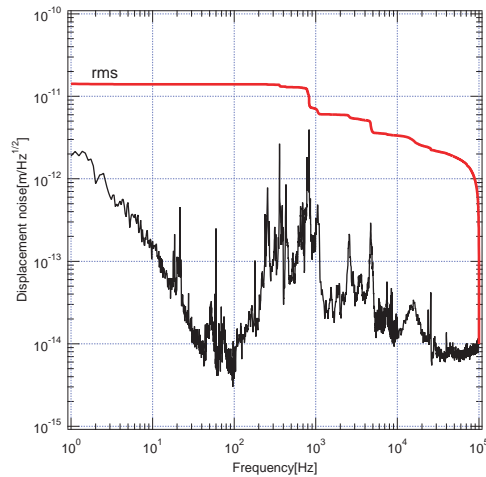


Figure 4. Mach Zehnder residual noise calibrated as fluctuations in the relative arm length.

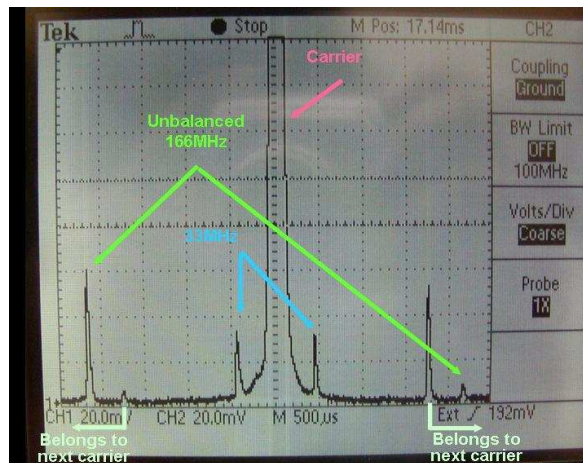


Figure 5. Frequency components of the modulated laser light measured on reflection from the interferometric system. There are no additional frequency components observed at the beat between the sideband frequencies. The unbalanced sidebands effect is due to the interaction of the light with the interferometer.

system uses one of sets of sidebands (f_1), detected at the unused Mach Zehnder dark port and demodulated, to derive a control signal which subsequently feeds back to a piezo-electric transducer (PZT) bonded to one of the mirrors. Fluctuations on the signal are calibrated to give the residual change in relative arm length (see Figure 4).

The residual noise of the Mach Zehnder can be seen to rise above $10^{-12} \text{ m}/\sqrt{\text{Hz}}$ in the several hundred Hz to 1 kHz region. With a 10% imbalance in ITM transmissivity the direct coupling mechanism will result in a detector sensitivity limit of around $10^{-18} \text{ m}/\sqrt{\text{Hz}}$ from the L_- sensing output. This is around 2 orders of magnitude higher than the design specification for the prototype system.

The performance of the Mach Zehnder servo loop could be easily improved by increasing the gain, but in the configuration shown, gain is limited by intrinsic resonances of the PZT.

The unity gain frequency of the loop is ~ 11 kHz. The servo bandwidth could be increased by inserting a phase correcting electro-optic modulator in one of the Mach Zehnder arms to feed back at higher frequencies and allowing the gain to be increased in the region of interest. Using this method the residual length fluctuations could be reduced by several orders of magnitude.

Using the Mach Zehnder parallel modulation scheme, sidebands have been generated without sidebands of sidebands (shown in Figure 5). The resulting length sensing signals have been used to lock the prototype interferometric system in a full Advanced LIGO configuration [11]. The work presented here demonstrates that, given a suitably high gain servo loop, the parallel modulation scheme is a viable option for the generation of control sidebands in full scale advanced interferometric gravitational wave detectors.

This work is supported by the Particle Physics and Astronomy Research Council and the University of Glasgow in the UK and from the National Science Foundation cooperative agreement PHY0107417. The authors also acknowledge the support of colleagues within the LIGO Science Collaboration (LSC).

References

- [1] Abramovici A *et al.*, 1992, *Science* **256** 325–333
- [2] Bradaschia C *et al.*, 1990, *Nucl. Instrum. Methods in Physics Research A* **289** 518–525
- [3] Danzmann K *et al.*, 1995, *1st Edoardo Amaldi Conf. on Gravitational Wave Experiments (Frascati, 1994)*, (Singapore: World Scientific) 100–111
- [4] Tsubono K *et al.*, 1995, *1st Edoardo Amaldi Conf. on Gravitational Wave Experiments (Frascati, 1994)*, (Singapore: World Scientific) 112–114
- [5] *An overview of gravitational-wave sources* in Proceedings of the GR16 Conference on General Relativity and Gravitation, N. Bishop, ed. (Singapore: World Scientific, 2002).
- [6] Gustafson E, Shoemaker D, Strain K and Weiss R, 1999, *LSC White Paper on Detector Research and Development*, LIGO Document T990080-00-D
- [7] Strain K A and Müller G and Delker T and Reitze D H and Tanner D B and Mason J E and Willems P A and Shaddock D A and Gray M B and Mow-Lowry C and McClelland D E, 2003, *App. Optics* **42** 1244–1256
- [8] Drever R W P and Hall J L and Kawalski F W and Hough J and Ford G M and Munley A J and Ward H, 1981, *App. Phys. B.* **31** 97–105
- [9] Freise A, *FINESSE - Frequency domain interferometer simulation software*
Available from <http://www.rzg.mpg.de/~adf/>
- [10] Kawamura S and Miyakawa O, 2004, *LIGO internal note*
Available from: <http://www.ligo.caltech.edu/~cit40m/Docs/T040166-00.pdf>
- [11] Miyakawa O *et al.*, 2006, *Measurement of Optical Response of a Detuned Resonant Sideband Extraction Interferometer*, (in preparation)